Journal of Magnetism and Magnetic Materials 324 (2012) 440–444

Contents lists available at SciVerse ScienceDirect

Journal of Magnetism and Magnetic Materials

journal homepage: www.elsevier.com/locate/jmmm

Effect of NiAl underlayer and spacer on magnetoresistance of current-perpendicular-to-plane spin valves using $Co_2Mn(Ga_{0.5}Sn_{0.5})$ Heusler alloy

N. Hase [a,b], T.M. Nakatani [a,b], S. Kasai [b], Y.K. Takahashi [b], T. Furubayashi [b], K. Hono [a,b,*]

[a] Graduate School of Pure and Applied Science, University of Tsukuba, Tsukuba 305-8577, Japan
[b] Magnetic Materials Unit, National Institute for Materials Science, Tsukuba 305-0047, Japan

ARTICLE INFO

Article history:
Received 9 April 2011
Available online 11 August 2011

Keywords:
Giant magnetoresistance
CPP-GMR
Spin valve
Heusler alloy

ABSTRACT

We investigated the effect of a NiAl underlayer and spacer on magnetoresistive (MR) properties in current-perpendicular-to-plane spin valves (CPP-SVs) using $Co_2Mn(Ga_{0.5}Sn_{0.5})$ (CMGS) Heusler alloy ferromagnetic layers. The usage of a NiAl underlayer allowed a high temperature annealing for the $L2_1$ ordering of the bottom CMGS layer, giving rise to a MR ratio of 10.2% at room temperature. We found that the usage of a NiAl spacer layer also improved the tolerance of the multilayer structure against thermal delamination, which allowed annealing to induce the $L2_1$ structure in both the bottom and top CMGS layers. However, the short spin diffusion length of NiAl resulted in a lower MR ratio compared to that obtained using a Ag spacer. Transmission electron microscopy of the multilayer structure of CPP-SVs showed that the atomically flat layered structure was maintained after the annealing.

1. Introduction

Current-perpendicular-to-plane giant magnetoresistance (CPP-GMR) devices using Heusler alloy ferromagnetic (FM) layers have attracted much interest recently for potential applications as read sensors [1–4] and spin torque oscillators [5–7] of future ultrahigh density hard disc drives (HDDs). Many recent investigations have shown that the magnetoresistive outputs of the spin valves using Heusler alloys are much larger than those obtained using conventional FM layers such as CoFe [8,9]. One of the reasons for the superior MR properties is the half-metallicity of the FM Heusler alloys as predicted by the density of state calculations [10–13]. The high spin polarizations of the Heusler alloys have also been demonstrated experimentally using magnetic tunnel junctions and CPP-GMR devices [14–19]. To extract the highly spin polarized current from the FM Heusler alloys, it is necessary to anneal sputter-deposited A2 or B2 films to obtain the $L2_1$ ordered structure typically above 400 °C. However, such high temperature annealing often leads to the degradation of MR properties due to the delamination of the layered thin films or the interdiffusion of alloying elements [4,19–21]. Indeed, we have observed the reduction of ΔRA in the CPP-GMR devices with $Co_2Mn(Ga_{0.5}Sn_{0.5})$ Heusler alloy layers and a Ag spacer layer by annealing above 450 °C, which was attributed to the destruction of the Heusler/Ag/Heusler trilayer structure by the annealing [21]. Hence, suppressing the degradation of the multilayered structure of the devices by annealing is essential for utilizing the full potential of FM Heusler alloys.

In this work, we present one solution for suppressing the degradation of the MR properties by annealing, *i.e.*, the use of a NiAl underlayer and spacer layer in CPP-GMR devices with a $Co_2Mn(Ga_{0.5}Sn_{0.5})$ (CMGS) Heusler alloy [21–23]. The B2 ordered phase of the NiAl intermetallic compound (lattice constant: 0.289 nm [24]) is stable up to the melting temperature of 1600 °C due to the large negative mixing enthalpy between Ni and Al. Thus, we can expect NiAl to be a promising material as a heat-resistant layer or a diffusion barrier by preventing the thermal delamination of the multilayer structure. In addition, the small lattice misfit of 2.2% for NiAl(001)[100]‖CMGS(001)[100] and 0.30% for NiAl(001)[100]‖Ag(001)[100] would result in the epitaxial growth of multilayer films. Although NiAl contains a ferromagnetic element, it is paramagnetic since the d-band of Ni is filled with electrons from Al [25]. Therefore, the NiAl phase can be used as a spacer as well as an underlayer in CPP-GMR devices. In fact, Nakatani et al. demonstrated that the pseudo-spin valve with a thin NiAl spacer shows comparable MR properties with that of a Ag spacer [22]. Moreover, a good band matching between NiAl and Heusler compounds has been implied [22], which should be effective for enhancing MR outputs as discussed by Ambrose et al. [26–28]. Hence, the combination of a NiAl spacer layer and a Heusler alloy layer is interesting from the point of band matching as well as the heat-resistance of the multilayer structure.

* Corresponding author at: Magnetic Materials Unit, National Institute for Materials Science, Tsukuba 305-0047, Japan.
E-mail address: kazuhiro.hono@nims.go.jp (K. Hono).

0304-8853/$ - see front matter © 2011 Elsevier B.V. All rights reserved.
doi:10.1016/j.jmmm.2011.08.012

2. Experiment

All the films were deposited on MgO(100) single crystalline substrates at room temperature with a UHV magnetron sputtering machine ($P_{base} < 2 \times 10^{-7}$ Pa). To investigate the effect of the NiAl underlayer on the B2 and $L2_1$ ordering, X-ray diffraction (XRD) measurements were carried out for the annealed MgO(001)/Cr(10 nm)/Ag(75 nm)/CMGS(20 nm)/Ru(2 nm) and MgO (001)/Cr(10 nm)/Ag(75 nm)/NiAl(10 nm)/CMGS(20 nm)/Ru(2 nm) films. These stacks of films were annealed at temperatures ranging from 400 °C to 600 °C. Inductively coupled plasma (ICP) analysis showed that the CMGS films had a stoichiometric composition close to $Co_{50.4}Mn_{24.8}Ga_{12.5}Sn_{12.3}$.

CPP spin valves (CPP-SVs) were prepared by microfabricating multilayer stacks of MgO(001)sub/Cr(10 nm)/Ag(75 nm)/NiAl (10 nm)/CMGS(20 nm)/Ag(5 nm)/CMGS(5 nm)/CoFe(2 nm)/IrMn (10 nm)/Ru(8 nm) and MgO(100)sub/Cr(10 nm)/Ag(75 nm)/NiAl (10 nm)/CMGS(20 nm)/NiAl(5 nm)/CMGS(5 nm)/CoFe (2 nm)/ IrMn(10 nm)/Ru(8 nm). To discuss the effectiveness of the NiAl underlayer, the results were compared to those obtained from similar stacks of films with the Ag underlayer and Ag spacer that were reported in our previous paper [21]. The bottom CMGS(20 nm) layer of the NiAl underlayers was annealed at various temperatures (T_{bottom}) from 400 °C to 600 °C. The top CMGS layers were also annealed at various temperatures (T_{top}) from 400 °C to 550 °C. The types of underlayers and spacers and the heat treatment temperatures are summarized in Table 1. After the depositions of all the layers, the stacks were annealed under a magnetic field of 5 kOe along the $[110]_{CMGS}$ axis to obtain an exchange bias field from the IrMn antiferromagnetic layer.

The films were patterned into pillars with four electrode terminals using photolithography, electron beam lithography and Ar ion milling. The shape of the pillar was designed as an ellipse with an aspect ratio of 2:1. The pillars ranged in size from 80 nm × 160 nm to 200 nm × 400 nm on one substrate. The actual sizes of the pillars after microfabrication were measured with a scanning electron microscope (SEM) to obtain an accurate estimation of the ΔRA value. The MR values were measured by the dc four-probe method. In addition, the structural analysis of the CPP-SVs was performed with a transmission electron microscope (TEM).

3. Results and discussion

Figs. 1(a) and (b) shows the XRD patterns of the θ–2θ (out-of-plane) scan from the (001) and (111) planes of the CMGS layers on a NiAl underlayer, *i.e.*, MgO(001)sub/Cr(10 nm)/Ag(75 nm)/NiAl (10 nm)/CMGS(20 nm)/Ru(2 nm). The film was post annealed at temperatures from 400 °C to 600 °C. The growth orientation of the CMGS layer deposited on the MgO (001) substrate was $(001)_{MgO} \parallel (001)_{CMGS}$ and $[100]_{MgO} \parallel [110]_{CMGS}$. The $\{200\}_{CMGS}$ peak indicating the B2 ordered structure was observed for all T_{PA}, while the $\{111\}_{CMGS}$ peak indicating the $L2_1$ ordered structure was only observed for $T_{PA} > 450$ °C as shown in Fig. 1(b), suggesting that the $L2_1$ ordering only progresses above $T_{PA} = 450$ °C. This ordering tendency of the CMGS layer on the NiAl underlayer is the same as that on the Ag underlayer [21]. Fig. 1(c) shows the variations of the integral intensity ratio of I_{200}/I_{400} for the B2 order and I_{111}/I_{444} for the $L2_1$ order as functions of T_{PA} ($T_{PA} = 0$ °C indicates the as-deposition state) for the samples with NiAl and Ag underlayers. There is not much difference between I_{200}/I_{400} for the CMGS layers on the NiAl and Ag underlayers, indicating that the underlayers do not have much influence on the kinetics for the B2 ordering. Note that the $L2_1$ order of the CMGS layer on the Ag underlayer was degraded when it was annealed above 500 °C. We believe that it is due to the interdiffusion between the Ag and CMGS layers. On the other hand, the intensity ratio I_{111}/I_{444} for the CMGS layer on the NiAl underlayer showed a maximum at 550 °C. This suggests that the NiAl underlayer is more suitable for achieving a higher degree of $L2_1$ order under a higher annealing temperature than that of the Ag underlayer.

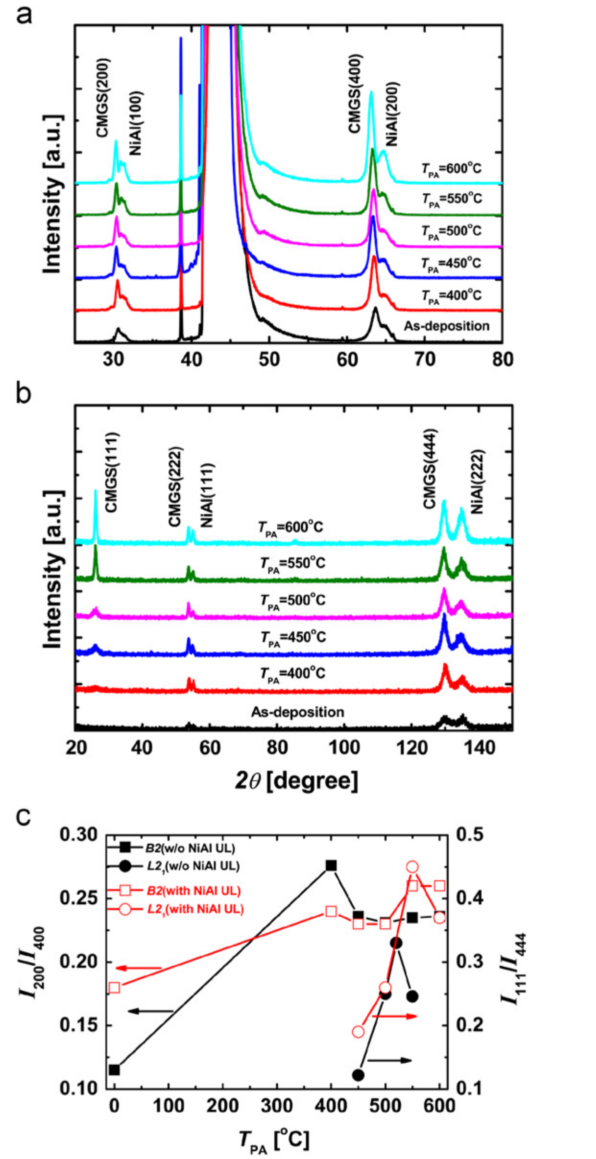

Fig. 1. X-ray diffraction (XRD) patterns of θ–2θ (out of plane) scans (a) from (001) and (b) from the (111) planes of the CMGS layer annealed at various temperature (T_{PA}) in a multilayer structure of MgO(001)sub/Cr(10 nm)/Ag(75 nm)/ NiAl(10 nm)/CMGS(20 nm)/Ru(2 nm). (c) Summary of the integral intensity ratio of B2 (I_{200}/I_{400}) (square) and $L2_1$ (I_{111}/I_{444}) (circle) versus T_{PA} ($T_{PA} = 0$ °C indicates As-deposition status.) in multilayer structures of MgO(001)sub/Cr(10 nm)/ Ag(75 nm)/ with (open square and open circle) or without (close square and close circle) NiAl(10 nm)/CMGS(20 nm)/Ru(2 nm).

Table 1
Summary of heat treatment temperatures for the bottom and top CMGS layers in several combinations of underlayer and spacer.

(UL/spacer)	T_{bottom} (°C)	T_{top} (°C)
(Ag/Ag)	400–520	400–520
(NiAl/Ag)	400–600	400
(NiAl/NiAl)	550	400–550